Polyelectrolyte membranes based on hydrocarbon polymer containing fullerene

Shota Saga, Hidetoshi Matsumoto, Keiichiro Saito,
Mie Minagawa, Akihiko Tanioka *

*Department of Organic and Polymeric Materials, Tokyo Institute of Technology, International Research Center
for Macromolecular Science, Mail Box S8-27, 2-12-1 Ookayama, Meguro-ku, Tokyo 152-8552, Japan*

Abstract

In the present study, composite polyelectrolyte membranes were prepared from sulfonated polystyrene and fullerene. The additive effect of the fullerene on the membrane properties – electric resistance, mechanical strength, oxidation resistance, and methanol permeability – were measured. The addition of fullerene improved the oxidation resistance, and reduced the methanol crossover. The mechanical strength of the fullerene-composite membrane, on the other hand, was not improved. The direct methanol fuel cell (DMFC) based on a 1.4 wt% fullerene-composite membrane showed the highest power density of 47 mW cm^{-2} at the current density of 200 mA cm^{-2} (this value is 60% of the Nafion-based DMFC). The transmission electron microscopy (TEM) observations suggest that the improved dispersity of the fullerene and the reduced number of micropores in the membranes would improve its performance in the fuel cell.
© 2007 Elsevier B.V. All rights reserved.

Keywords: Polyelectrolyte membrane; Hydrocarbon polymer; Polystyrene; Fullerene; Direct methanol fuel cell; Oxidation resistance

1. Introduction

The polyelectrolyte membrane has attracted much attention due to their promising applications in polymer electrolyte fuel cells (PEFCs) [1] and direct methanol fuel cells (DMFCs) [2]. Perfluorosulfonated membranes (e.g., Nafion®, Flemion®, Aciplex-F®) are widely used for polyelectrolyte membranes, due to their excellent chemical stability and high proton conductivity [3]. The major disadvantages of these membranes, however, are their high cost and low recycling properties of the fluorinated polymers. In addition, perfluorosulfonated membrane shows a low DMFC performance due to the methanol crossover [4]. Based on these characteristics, hydrocarbon polyelectrolyte membranes, which are low cost, disposable, and have a low methanol permeability, have been required as an alternative polyelectrolyte membrane.

Recently, many kinds of hydrocarbon polyelectrolyte membranes, such as sulfonated polybenzimidazole (PBI) [5], sulfonated poly(ether ether ketone)s (PEEKs) [6], sulfonated poly(sulfone)s [7,8] and sulfonated polyimides [9], have been reported. Our previous study reported the preparation of sulfonated syndiotactic polystyrene (semicrystalline polymer based on the stereoregular structure shown in Fig. 1 [10]) membranes and their better conductivity and mechanical strength than the perfluorosulfonated membrane [11]. However, it has been pointed out that the durability of a hydrocarbon polyelectrolyte membrane is still not adequate. The formation of reactive oxygen species by the catalytic process during PEFC operation has been demonstrated [12–14]. H$_2$O$_2$ and HO$^{\bullet}$ are the most commonly reported species and their presence induces membrane degradation. We have attempted to add a radical scavenger to the hydrocarbon polyelectrolyte in order to improve the oxidation resistance of the membrane. It is well known that C$_{60}$ easily reacts with low-molecular-weight alkyl radicals that forms remarkably persistent products R$_n$C$_{60}$ (where $n = 1, 2, 3,...$) [15,16]. Recently, Troitskii et al. showed that fullerene C$_{60}$ retards the thermo-oxidative

* Corresponding author. Tel.: +81 3 5734 2426; fax: +81 3 5734 2876.
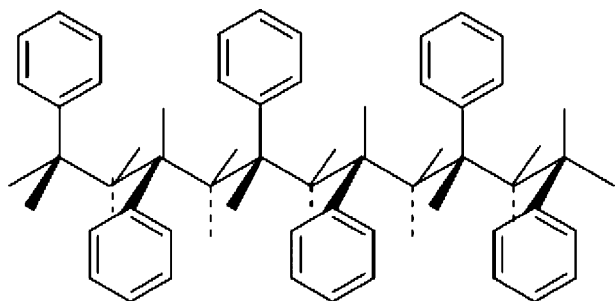 *E-mail address:* tanioka.a.aa@m.titech.ac.jp (A. Tanioka).

Fig. 1. Chemical structure of syndiotactic polystyrene.

degradation of poly(methyl methacrylate) and polystyrene [17].

In the present study, we prepared a fullerene-sulfonated polystyrene composite membrane and investigated the addition effect of the fullerene on the oxidation resistance, mechanical strength, and methanol permeability. Moreover, the DMFC performance was also evaluated.

2. Experimental

2.1. Materials

Atactic polystyrene (aPS, $\overline{M_W} = 300,000$) and syndiotactic polystyrene (sPS, $\overline{M_W} = 320,000$, crystallinity = 42%, tacticity = 99%) were kindly supplied by Idemitsu Kosan, Japan. The fullerene (mixture of C_{60} and C_{70}; C_{60}:C_{70} = 5:2 in weight) was purchased from Frontier Carbon Corporation, Japan. 1,2-Dichlorobenzene (DCB, b.p.: 180–183 °C) of ultra-pure grade was purchased from Wako Pure Chemicals Industries, Japan. All reagents were used without further purification.

2.2. Membrane preparation and characterization

A solution casting was used to prepare the membranes. The mixture of aPS and sPS (aPS: 1.4 g, sPS: 5.6 g, aPS/sPS = 2/8 w/w) were dissolved in DCB at 160 °C. After cooling the solution to 120 °C, 97% H_2SO_4 (1.4 mL) was added to the solution for the sulfonation of PS and then a 20 mg mL^{-1} fullerene/DCB solution was added to the solution (total DCB volume is fixed at 4.5 mL). After stirring the solution for 2 h, the solution was cast onto a polytetrafluoroethylene (PTFE)-coated glass plate and then dried at 100 °C for 12 h. The prepared membranes were thoroughly washed with deionized water. The composition of the prepared membranes is listed in Table 1.

Table 1
Composition of prepared membranes

Membrane	aPS (wt%)	sPS (wt%)	Flu (wt%)
PS	20	80	–
0.57% Flu-PS	20	80	0.57
1.4% Flu-PS	20	80	1.4
2.8% Flu-PS	20	80	2.8

aPS: atactic polystyrene; sPS: syndiotactic polystyrene; Flu: fullerene.

The potentiometric titration was performed using an automatic titrator (DMS Titrino 716, Metrohm, Switzerland) connected to a combined pH glass electrode (#6.0218.010, Metrohm, Switzerland) as previously described [18]. Two pieces of the test membrane (each membrane area was 4 cm × 4 cm) were immersed in 2 mol L^{-1} HCl for 12 h in order to convert the counterion to the H$^+$ form. They were then sufficiently washed with deionized water. Thereafter, the membranes were immersed in 50 mL of 2 mol L^{-1} KCl with stirring for 1 h. These treatments were repeated four times in order to thoroughly elute the H$^+$ from the membranes, and all eluents were then collected. The collected solutions were titrated with 0.1 mol L^{-1} KOH. The titers of KOH correspond to the amount of fixed-charge groups in the test membrane, N_X (mol). The weight of the equilibrium swollen membrane, w_{wet} (g), was measured after carefully removing the surface water with filter paper; and the weight of the dried membrane, w_{dry} (g), was measured after vacuum-drying at 100 °C for 6 h. The equilibrium water content of the membranes, w_w (%), is given by

$$w_w = \frac{w_{wet} - w_{dry}}{w_{wet}} \times 100 \tag{1}$$

The ion-exchange capacity, IEC (equiv. g^{-1}-dry membrane), and the fixed-charge density, C_X (mol L^{-1}), are determined by using the following equations:

$$IEC = \frac{N_X}{w_{dry}} \tag{2}$$

$$C_X = \frac{\rho N_X}{w_{wet} - w_{dry}} \tag{3}$$

where ρ is the density of water at 25 °C (=0.99704 × 10^3 g L^{-1}).

All measurements were carried out at 25 ± 1 °C.

The electric resistance of the prepared membranes was measured by the ac-impedance method. The apparatus, which is composed of an impedance analyzer (HP4192A, Agilent, USA) and the measurement cell, is the same as that used in a previous study [19]. The measurement cell consisted of a pair of Pt-black coated Ti electrodes whose area is 1.0 cm^2. A 0.5 mol L^{-1} HCl solution was used for the measurement. The membranes were immersed in a 2 mol L^{-1} HCl solution for 1 day to exchange their counter ions for H$^+$, and then they were thoroughly washed with deionized water. The membranes (effective area is 1.0 cm^2) in the equilibrium state were placed between the electrodes, and then their electric resistances, R_{meas}, were measured. The frequency ranged from 100 Hz to 10 kHz. Next, when there was no membrane between the electrodes, the electric resistance, R_{soln} was measured. The specific resistance of the membrane, ρ, was calculated using the following equations:

$$S = \frac{d}{\kappa R_{soln}} \tag{4}$$

$$\rho = (R_{meas} - R_{soln}) \frac{S}{d_{mem}} \tag{5}$$

where S is the effective area of the membrane, d is the distance between the electrodes, κ is the electric conductivity of the 0.5 mol L^{-1} HCl solution, and d_{mem} is the thickness of the membrane.

The morphologies of the prepared membranes were observed using a scanning electron microscope (SEM, SM-200, Topcon, Japan). All samples were sputter-coated with Au. To evaluate the microstructure of the prepared membranes, a thin sample with thickness of 50 nm was cut from the bulk of the membrane. The sample was examined using a transmission electron microscope (TEM, JEM-200CX, JEOL, Japan).

The mechanical properties were measured using a universal testing machine (3342, Instron, USA) under a crosshead speed of 4 mm min^{-1} at room temperature. The test specimens were cut into a dumbbell shape; the specimen had a width of 2 mm and a gauge length of 10 mm.

The oxidation resistance of the prepared membranes was evaluated by Fenton's test [20]. Fenton's reagent was prepared from a 3 wt% H$_2$O$_2$ aqueous solution containing 10 ppm FeSO$_4$. The test membranes were immersed in Fenton's reagent solution with stirring at 60 °C for 1–3 h. The weight loss of the membranes was then measured.

2.3. DMFC performance and methanol permeability

Fig. 2 shows a schematic diagram of the DMFC and methanol permeation measurement. A DMFC generating unit (HDM-1000, Eiwa, Japan) and Japan Automobile Research Institute (JARI) standard cell (Ex-1, EIWA, Japan) were used. The membrane/electrode assemblies were formed by hot-pressing the electrodes onto a membrane sample at 165 °C and at a
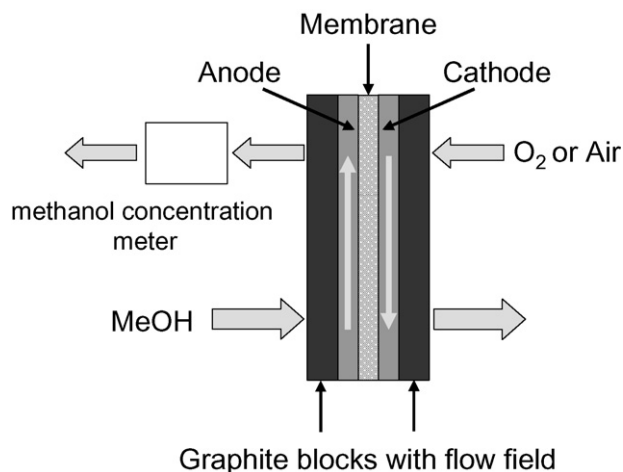
Fig. 2. Schematic representation of DMFC and methanol permeation measurements.

pressure of 46 kg cm^{-2} for 10 min. The Pt–Ru/C catalyst (Pt 1.02 mg cm^{-2}) and the Pt/C catalyst (Pt 1.00 mg cm^{-2}) were used for the anode and cathode, respectively. Nafion was impregnated into each electrode. The temperature of the cell was 80 °C. Dried O$_2$ gas was supplied to the cathode at 400 mL min^{-1}. A 1 mol L^{-1} MeOH aqueous solution was supplied to the anode at 2.5 mL min^{-1}.

The MeOH permeation measurements in the liquid phase were also carried out at 80 °C using the DMFC cell and non-catalyzed membranes. Dried air was fed into the cathode at 150 mL min^{-1}. A 1 mol L^{-1} MeOH aqueous solution was fed into the anode at 1.5 mL min^{-1}. The MeOH permeation flux was determined from the concentration change between the inlet and
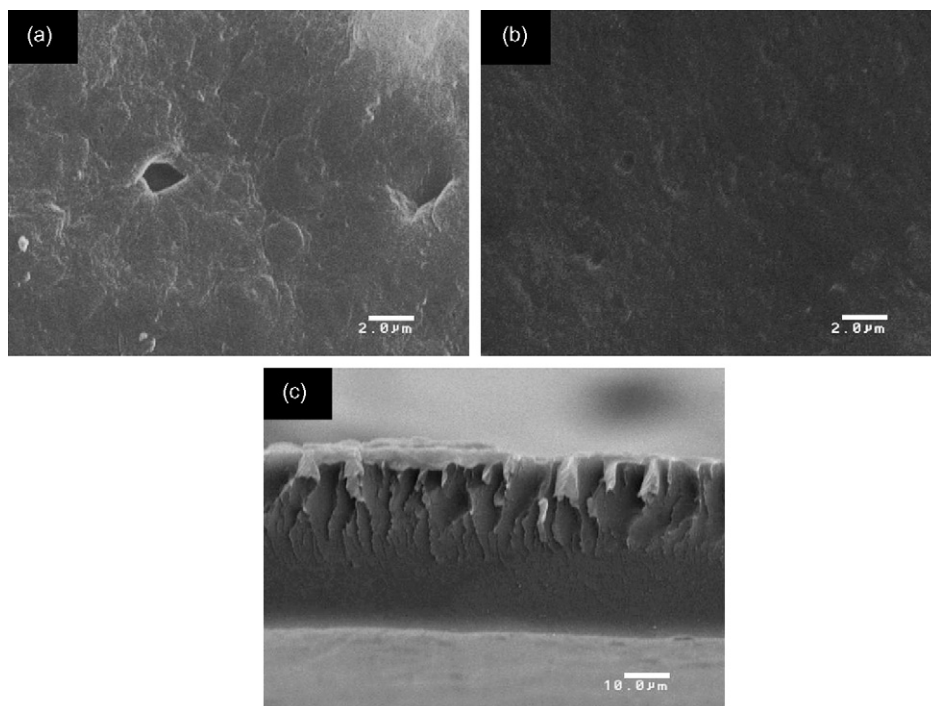
Fig. 3. SEM images of fullerene-sulfonated polystyrene composite membrane (1.4% Flu-PS): (a) air-side surface; (b) substrate-side surface; (c) cross-section (top surface is air-side surface).
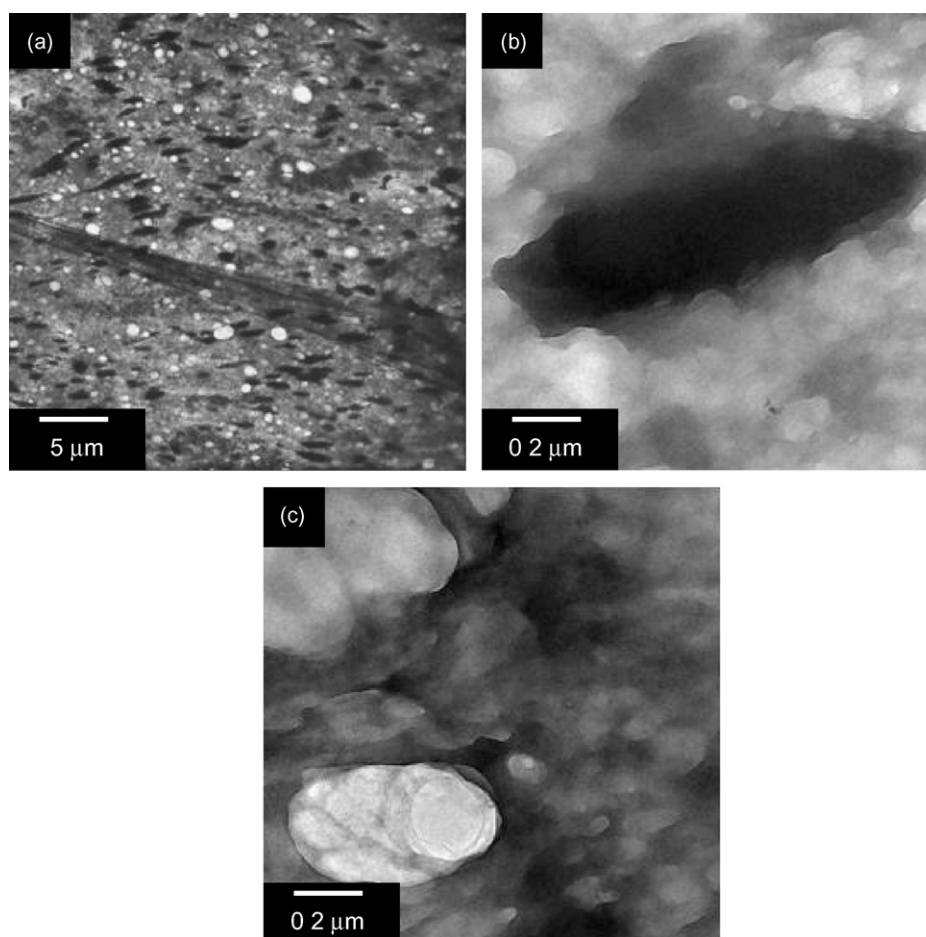
Fig. 4. TEM images of fullerene-sulfonated polystyrene composite membrane (1.4% Flu-PS): (a) bulk of prepared membrane; (b) fullerene region of (a) with high magnification; (c) micropore region of (a) with high magnification.

outlet of the anode of the DMFC. The concentration of MeOH was measured using a methanol concentration meter (FCD-200, EIWA, Japan).

3. Results and discussion

3.1. Membrane preparation and characterization

We grew the fullerene-sulfonated polystyrene composite membranes by the solution-casting method from the solutions with different fullerene concentration between 0 and 2.8 wt%. All the fullerene-composite membranes are transparent and brown colored, and the color of the higher fullerene-content membrane was darker. On the other hand, the sulfonated polystyrene membrane without fullerene is transparent and white colored.

Figs. 3 and 4 display the typical SEM and TEM images of the fullerene-sulfonated polystyrene composite membranes, respectively. The SEM images demonstrated that the membrane had a homogeneous surface structure and cross-sectional asymmetric structure (Fig. 3). The TEM images show a comparatively uniform distribution of the black and white areas. In Fig. 4, the black area with a high electron density in the images is part of the fullerene agglomerate (the size of agglomerate is

approximately 1 μm, while the diameter of fullerene is about 0.7 nm). The size of the agglomerate does not contradict the color of the fullerene-sulfonated polystyrene composite membranes by visual observations. On the other hand, the white area with a low electron density in the images is the part of the pores (the size of approximately 0.5 μm). It would be formed by the existence of air bubbles trapped in the viscous casting solution.

Table 2 shows the physicochemical properties – ion-exchange capacity, fixed-charge density, specific resistance, water content, and thickness – of the prepared membranes. The commercial perfluorosulfonated ionomer membrane (Nafion 117, Du Pont, USA) was used for comparison. All the fullerene-composite membranes showed around a 2.5 mequiv. g^{-1}-dry membrane ion-exchange capacity and around a 17 Ω cm specific resistance. These values correspond to those of the membrane without fullerene. Thus, the addition of fullerene did not reduce the electrochemical properties of the PS membrane. The specific resistance of the prepared membranes was 50% higher than that of Nafion 117. The water content of the prepared membranes showed a 90–100%. The values correspond to that of the PS membrane and were 3–4 times higher than that of Nafion 117. This would be attributed to the existence of "micropores" in the membrane observed by TEM. Moreover, the addition of

Table 2
Physicochemical properties of prepared membranes

Membrane	IEC (mequiv. g^{-1}-dry memb.)	C_X (mol L^{-1})	ρ (Ω cm)	w_w (w/w%)	Thickness (μm)
PS	2.5	2.7	16	91	114
0.57% Flu-PS	2.5	2.5	18	100	129
1.4% Flu-PS	2.6	2.6	17	100	94
2.8% Flu-PS	2.3	2.5	17	93	96
Nafion 117	1.0	3.7	11	27	210

IEC: ion-exchange capacity; C_X: fixed-charge density; ρ: specific resistance; w_w: water content. Nafion 117, commercial perfluorosulfonated membranes, from Du Pont, USA.

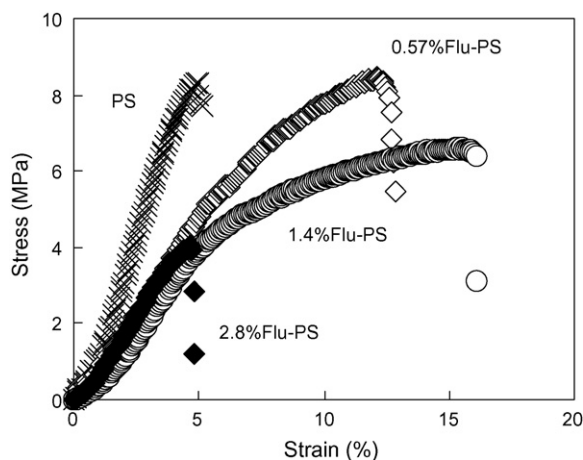Fig. 5. Stress–strain curves of fullerene-sulfonated polystyrene composite membranes.

Fig. 6. Oxidation resistance of fullerene-sulfonated polystyrene composite membranes.

fullerene does not contribute to reduce the water content of the membranes.

Fig. 5 illustrates the stress–strain curves of the prepared membranes with the same dimensions. The mechanical properties of the prepared membranes are summarized in Table 3. All the prepared membranes with and without fullerene showed a much lower strength and strain at break than Nafion 117. The rupture stress and strain of the prepared membranes were 3–7 MPa and 4–16%, respectively; while those of Nafion 117 were 41 MPa and 328%, respectively. This would be attributed to the existence of "micropores" in the membrane as mentioned above. The addition of fullerene does not contribute to improving the mechanical strength of the membranes. The addition of a higher amount of the fullerene made the membrane more brittle. The Young's modulus, rupture stress, and maximum stress of the membranes decreased with an increase in the fullerene content in the membranes (Young's modulus decreased from 1.6 to 1.1 MPa, rupture stress decreased from 8.7 to 3.5 MPa, and max-

imum stress decreased from 9.5 to 4.3 MPa; when the content of fullerene increased from 0.57 to 2.8%). This would be attributed to the micro-scaled agglomerates of fullerene in the membranes (TEM images supported the fact that larger-scaled agglomerates were formed in the higher fullurene-content membrane).

Fig. 6 shows the results of the oxidation decomposition experiments using the fullerene-sulfonated polystyrene composite membranes. After 3 h, the 1.4 and 2.8% Flu-PS membranes maintained their structure. The PS membrane and the 0.57% Flu-PS membrane, on the other hand, were totally decomposed after 2.5 and 3 h, respectively. A larger amount of the fullerene-composite membrane showed a lower weight loss. We verified that the addition of fullerene was effective for improving the oxidation resistance of the membrane. This also suggested that HO$^{\bullet}$ was effectively trapped by the fullerene in the membrane as follows:

Table 3
Mechanical properties of prepared membranes

Membrane	Young's modulus (MPa)	Rupture stress (MPa)	Maximum stress (MPa)	Rupture strain (%)
PS	2.1	7.1	7.2	4.4
0.57% Flu-PS	1.6	8.7	9.5	11
1.4% Flu-PS	1.0	6.2	6.4	16
2.8% Flu-PS	1.1	3.5	4.3	7.3
Nafion 117	2.6	41	41	328

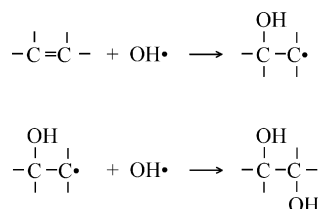Nafion 117, commercial perfluorosulfonated membranes, from Du Pont, USA.

Table 4
Methanol permeability of prepared membranes

Membrane	Permeability coefficient at 80 °C ($\times 10^{-6}$ cm^2 s^{-1})
PS	2.9
0.57% Flu-PS	2.1
1.4% Flu-PS	1.6
2.8% Flu-PS	1.5
Nafion 117	2.2

Nafion 117, commercial perfluorosulfonated membranes, from Du Pont, USA.

$$-\overset{|}{\underset{|}{C}}=\overset{|}{\underset{|}{C}}- \;+\; OH\bullet \;\longrightarrow\; -\overset{|}{\underset{|}{C}}-\overset{OH}{\underset{|}{C}}\bullet$$

$$-\overset{OH}{\underset{|}{C}}-\overset{|}{\underset{|}{C}}\bullet \;+\; OH\bullet \;\longrightarrow\; -\overset{OH}{\underset{|}{C}}-\overset{OH}{\underset{|}{C}}-$$

We believe that the addition of not only fullerene but also other radical scavengers to polyelectrolyte membranes was promising approach for improving the oxidation resistance of the membrane.

3.2. Methanol permeability and DMFC performance

The MeOH permeability through the prepared membranes measured using the DMFC cell is summarized in Table 4. The fullerene-composite membranes showed a lower MeOH permeability than the PS membrane. Specially, the MeOH permeability of the 1.4% Flu-PS and 2.8% Flu-PS membranes was 50% lower than that of the PS membrane. In addition, the 1.4% Flu-PS and 2.8% Flu-PS membranes showed a 30% lower permeability than Nafion 117. This would be attributed to the micro-scaled agglomerates of fullerene in the membranes. It is often observed that inorganic fillers such as SiO_2 can reduce the MeOH crossover [21]. The PS membranes, on the other hand, showed a higher MeOH permeability than Nafion 117. This would be attributed to the existence of "micropores" in the prepared membrane as mentioned in the previous section.

The 1.4% Flu-PS membrane was then used as the polyelectrolyte membrane for the DMFC performance test. This membrane has a comparably good proton conductivity and mechanical strength, along with a low methanol permeability in the fullerene-composite membranes. Fig. 7 shows the DMFC performance using the 1.4% Flu-PS membrane and Nafion 117 membrane operated at 80 °C. Although the MeOH permeability through the 1.4 wt% Flu-PS membrane was lower than that of Nafion 117, the 1.4 wt% Flu-PS membrane resulted in a lower open-circuit voltage than Nafion 117. This membrane also showed the highest power density of 47 mW cm^{-2} at the current density of 200 mA cm^{-2} (this value is 60% of the Nafion 117-based DMFC). This would be attributed to the higher resistance of the 1.4 wt% Flu-PS membrane than that of the Nafion (17 Ω cm vs. 11 Ω cm, see Table 2). We think that further reduction in methanol permeability is required for improvement of the DMFC performance based on fullerene-sulfonated polystyrene composite membrane.
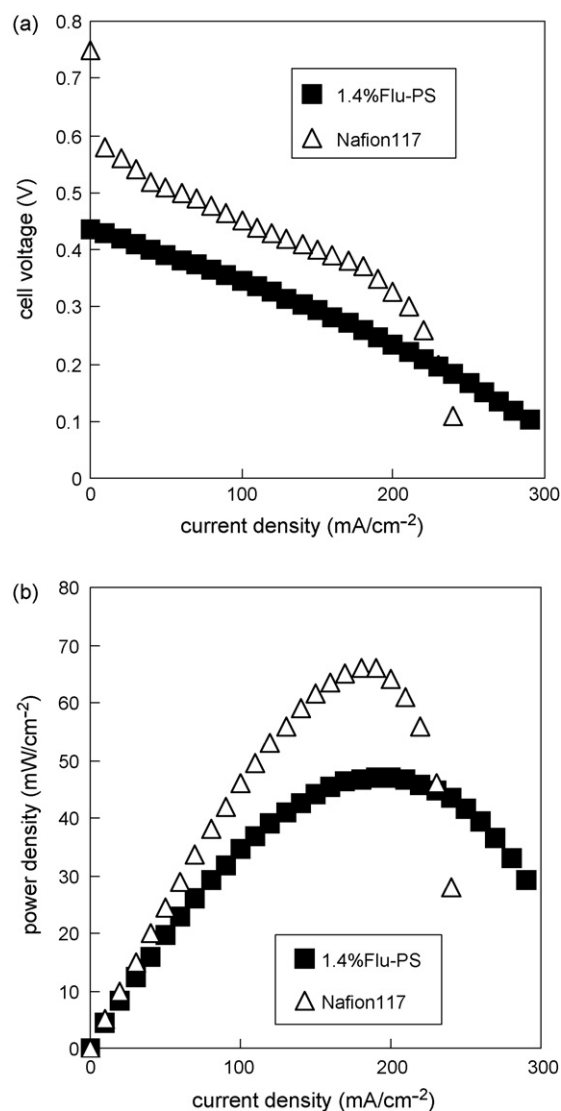

Fig. 7. DMFC performance of fullerene-sulfonated polystyrene composite membrane (1.4% Flu-PS): (a) cell voltages vs. electric current curves and (b) power density vs. electric current curves.

4. Conclusions

A fullerene-sulfonated polystyrene composite membrane was prepared by the solution-casting method. The addition of fullerene improved the oxidation resistance and reduced the methanol crossover. The former would be due to radical scavenging by the fullerene, and the latter would be due to the comparatively uniform dispersion of micro-scaled fullerene agglomerates in the bulk of the membrane. The mechanical strength of the fullerene-composite membrane, on the other hand, was not improved. The direct DMFC based on a 1.4 wt% fullerene-composite membrane showed the highest power density of 47 mW cm^{-2} at the current density of 200 mA cm^{-2} (this value is 60% of the Nafion-based DMFC).

We recognize that a polyelectrolyte membrane based on a fullerene-composite hydrocarbon in the present study is still under development. Our results suggest that the improved dispersity of fullerene on a nanoscale and the reduction of

micropores in the bulk of the membranes would produce a higher mechanical strength, higher oxidation resistance, and better DMFC performance caused by reduction in the methanol permeability.

Acknowledgement

References

[1] J. Larmine, A. Dicks, Fuel Cell Systems Explained, 2nd ed., Wiley & Sons, Chichester, 2003.

[2] X. Ren, P. Zelenay, S. Thomas, J. Davey, S. Gottesfeld, J. Power Sources 86 (2000) 111–116.

[3] M. Saito, N. Arimura, K. Hayamizu, T. Okada, J. Phys. Chem. B 108 (2006) 16064–16070.

[4] T. Yamaguchi, H. Zhou, S. Nakazawa, N. Hara, Adv. Mater. 19 (2007) 592–596.

[5] M. Kawahara, M. Rikukawa, K. Sanui, N. Ogata, Solid State Ionics 136/137 (2000) 1193–1196.

[6] L. Li, J. Zhang, Y. Wang, J. Membr. Sci. 226 (2003) 159–167.

[7] R. Nolte, K. Ledjeff, M. Bauer, R. Mulhaupt, J. Membr. Sci. 83 (1993) 211–220.

[8] L.E. Karisson, P. Jannasch, J. Membr. Sci. 230 (2004) 61–70.

[9] J. Fang, X. Guo, S. Harada, T. Watari, K. Tanaka, H. Kita, K. Okamoto, Macromolecules 35 (2002) 9022–9028.

[10] N. Ishihara, M. Kuramoto, M. Uoi, Macromolecules 21 (1988) 3356–3360.

[11] K. Saito, H. Takahashi, H. Matsumoto, M. Minagawa, A. Tanioka, Polym. Preprints, Jpn. 54 (2005) 4537–4538.

[12] T.J. Schmidt, U.A. Paulus, H.A. Gasteiger, R.J. Behm, J. Electroanal. Chem. 508 (2001) 41–47.

[13] C. Lu, C. Rice, R.I. Masel, P.K. Babu, P. Waszczuk, H.S. Kim, E. Oldfiled, A. Wieckowski, J. Phys. Chem. B 106 (2002) 9581–9589.

[14] A. Panchenko, H. Dilger, J. Kerres, M. Hein, A. Ullrich, T. Kaz, E. Roduner, Phys. Chem. Chem. Phys. 6 (2004) 2891–2894.

[15] P.J. Krusic, E. Wasserman, B.A. Parkinson, B. Malone, E.R. Holler Jr., P.N. Keizer, J.R. Morton, K.F. Preston, J. Am. Chem. Soc. 113 (1991) 6274–6275.

[16] J.R. Morton, K.F. Preston, P.J. Krusic, S.A. Hill, E. Wasserman, J. Am. Chem. Soc. 114 (1992) 5454–5455.

[17] B.B. Troitskii, L.S. Troitskaya, A.A. Dmitriev, A.S. Yakhnov, Eur. Polym. J. 36 (2000) 1073–1084.

[18] H. Matsumoto, R. Yamamoto, A. Tanioka, J. Phys. Chem. B 109 (2005) 14130–14136.

[19] N. Kimura, H. Matsumoto, Y. Konosu, R. Yamamoto, M. Minagawa, A. Tanioka, J. Colloid Interf. Sci. 286 (2005) 288–293.

[20] A. Bosnjakovic, S. Schlick, J. Phys. Chem. B 108 (2005) 4332–4337.

[21] P.L. Antonucci, A.S. Arico, P. Creti, E. Rammunni, V. Antonucci, Solid State Ionics 125 (1999) 431–437.